EPJ Web of Conferences **106**, 03005 (2016)
DOI: 10.1051/epjconf/201610603005

Assessing Pathways to Tritium Production and its Detailed Spatial Distribution Throughout the VHTR

Timothy Flaspoehler[a] and Bojan Petrovic

Georgia Institute of Technology, Nuclear and Radiological Engineering, 770 State St., Atlanta GA 30332-0745, USA

Abstract. The content of this work focused on calculating tritium production in the active core region as well as the surrounding components of the Very High Temperature Reactor (VHTR) using detailed Monte Carlo (MC) simulations. This is one of VHTR operational issues that need to be addressed. Permeation models of tritium in the VHTR plant have high levels of uncertainty associated with the initial tritium source from different pathways. In the past, the sources were generally derived from simple neutronics calculations in one dimension and one group. While providing a good estimate for integral pathways such as ternary fission, quantifying system-wide production via impurities in surrounding components may be largely inaccurate. To reduce this inaccuracy, the MAVRIC sequence of the SCALE 6.1 code package was used to calculate tritium production rates using a highly detailed Monte-Carlo model for neutron transport simulations covering the whole volume inside the reactor pressure vessel. It was found that assumptions about impurity concentrations in the graphite reflector and helium coolant could lead to larger tritium production rates than previously assumed from more simplified neutronics models. Previous studies showed that tritium permeation to secondary systems already exceeded EPA standards. Using a more detailed neutronics/shielding model in this study, even higher production rates were calculated than before. Based on these results, more work needs to be done to reduce leakage to secondary systems by improving helium purification systems and reducing impurities in structural components. Sophisticated transport theory simulations are necessary to support such analyses. The knowledge obtained in this study will also be used in tritium production studies related to liquid salt cooled reactors (LSCRs). Finally, it will inform design and selection of appropriate dosimetry needed to validate simulations.

1. Introduction

The VHTR design is slated to supply a heat source to different industrial applications including hydrogen production. If tritium leakage to secondary systems is above Environmental Protection Agency (EPA) standards, the industrial side of the plant would then need to be licensed by the Nuclear Regulatory Commission (NRC). From an economics standpoint this would be very costly to the company using the process heat and would likely deter investment in the technology. According to a

[a] Corresponding author: timothy.flaspoehler@gatech.edu

Table 1. Core isotopics used in the model.

	Fuel Compacts	Burnable Absorbers	Core Graphite
U-234	5.15669E-07	–	–
U-235	6.71673E-05	–	–
U-238	5.73317E-04	–	–
O-16	9.61500E-04	–	–
C-graphite	6.16851E-02	6.24123E-02	8.72433E-02
B-10	4.36000E-07	1.58597E-04	4.36000E-07
B-11	–	1.60337E-05	–
Li-6	–	–	7.50000E-08
Li-7	–	–	9.25000E-07
Si	2.74368E-03	–	–

report [1] released by INL in March of 2011 tritium generation in the core needs to be more accurately estimated in order to improve the overall contamination models for the entire industrial process side of the theoretical plant. Another study [2] done in 2007 claims that the production rates followed by permeation would cause a level of contamination above regulatory standards.

Tritium (^{3}H) is a radioactive isotope of the hydrogen atom with a half-life of over 12 years that decays by emitting an 18.590 keV beta particle. Being an isotope of the lightest element, tritium is difficult to contain within most atomic lattices and this effect is greatly enhanced by high temperature and radiation-induced damage within the core. Therefore, it is of special concern due to its permeation through structural materials and eventual leakage into the secondary systems and out into environment. Permeation models of tritium in the VHTR plant have very high levels of uncertainty as it is requires simulating many different time-dependent physical phenomena. One of the large areas of uncertainty is the tritium source description from core components. In this study, the MAVRIC sequence was used to calculate accurate and detailed production rates within all components inside the Reactor Pressure Vessel (RPV) using a detailed 3D model.

2. VHTR Model Basis

The General Atomics (GA) Gas Turbine-Modular Helium Reactor (GT-MHR) was one of the two leading designs chosen for the VHTR/NGNP project. The VHTR model used in this study primarily comes from the "NGNP and Hydrogen Production Preconceptual Design Studies Report" presented by General Atomics for the Battelle Energy Alliance, LLC [3]. Some assumptions have been made that may not be consistent with the current design, but are assumed to have little effect on the results of overall tritium production. The 600 MWth, annular core is graphite-moderated and helium-cooled. The active region consists axially of 10 layers of prismatic blocks with the radial layout shown in Fig. 1. The fuel blocks consist of fuel compacts, coolant holes and burnable poisons distributed in graphite. The coolant holes are distributed so that there is 1 coolant channel for every 2 fuel compact channels. At each corner there is a hole for a Lumped Burnable Poison (LBP) and the center has a hole for handling the elements, which is filled with graphite plugs. Additionally, the inlet and outlet plena are shown in Fig. 2. These areas contain the largest volume of helium which is one of the pathways of tritium production [4–6].

The core design in terms of fuel and absorbers has seen many variations adding to the large uncertainty in tritium production. Ternary fission in the fuel and tritium-producing reactions in the boron absorbers are considered to be the largest contributors. Therefore, carefully selected material compositions needed to be used and are based on personal communications with Dan Ilas [7] on a 1/6th-core 2D depletion study. The isotopics is given in Table 1 and includes lithium and boron impurities in graphite. Additionally, the annular control rods are made of B_4C granules in a graphite matrix formed into compacts, similar to the fuel pins. The compacts are 40% B_4C by weight, and the B_4C is enriched to 90% ^{10}B. The remaining 60% is graphite.

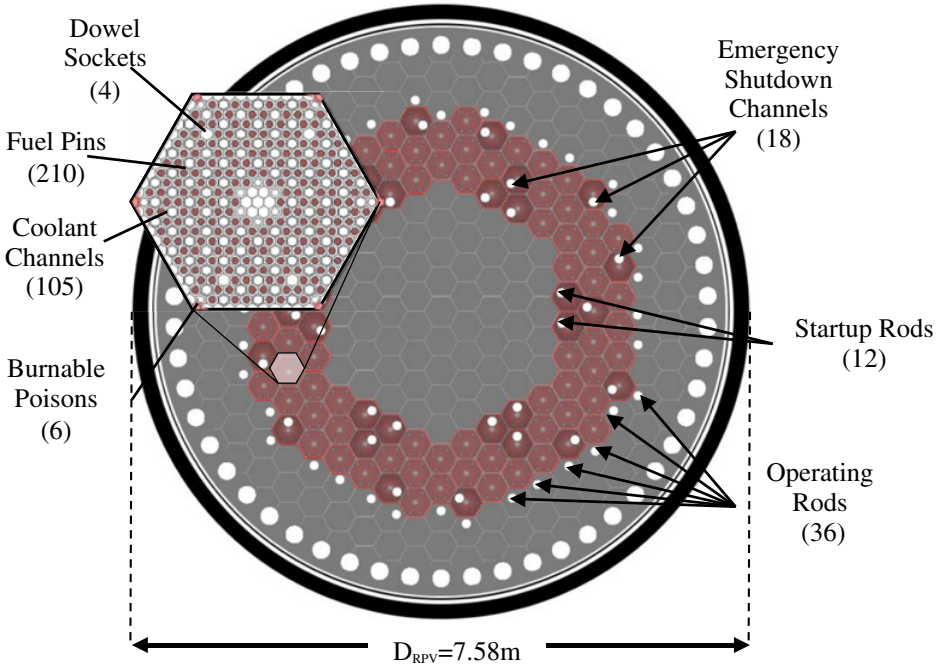

Figure 1. Radial layout of the VHTR core model through the RPV as implemented in the SCALE 6.1 model.

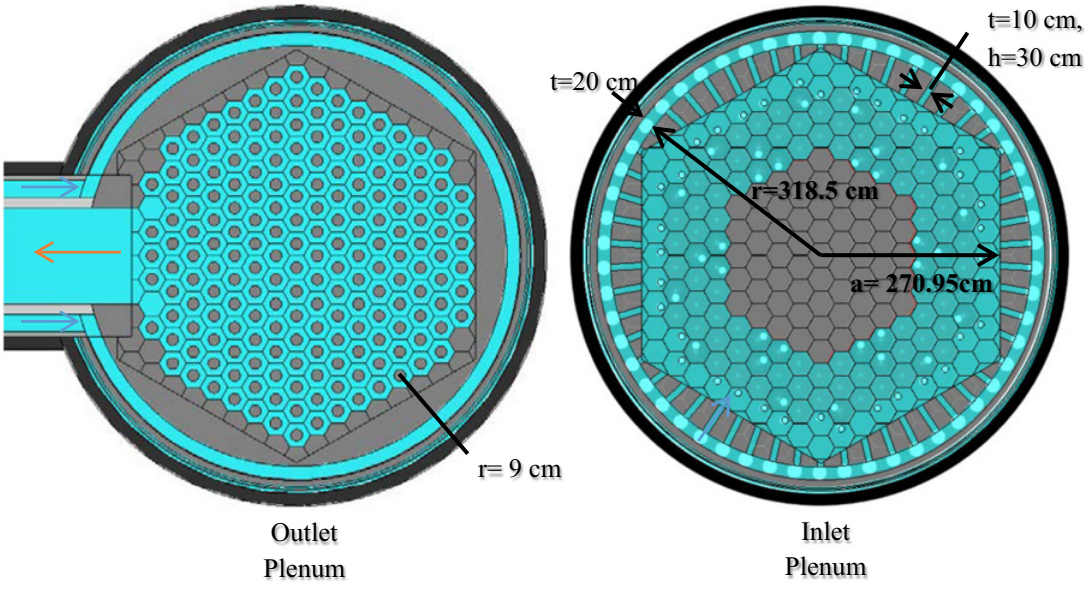

Figure 2. A radial view (left) of the outlet plenum below the active core region compared with a view (right) of the inlet plenum directly above the active core.

Table 2. Pathways of Tritium Production in the VHTR.

Process	MT #	Availability within SCALE 6.1
Ternary Fission	18 (x%yield)	YES
^{6}Li (n, α) ^{3}H or	107	NO
^{6}Li (n, t) ^{4}He	105	YES
^{7}Li (n, nα) ^{3}H or	22 / 105	NO / NO
^{7}Li (n, nt) ^{4}He or	33	NO
^{7}Li (n, Xt)		*YES
^{3}He (n, p) ^{3}H	103	YES
^{10}B (n, 2α) ^{3}H or	108	NO
^{10}B (n, t2α)	113	YES
^{10}B (n, α) ^{7}Li (n, Xt)	107 & 22	YES & NO

* Indicates taken from JENDL-4.0.

3. Pathways of Tritium Production

In previous studies, tritium production in the VHTR is assumed to be dominated by ternary fission in the fuel. Other systematic pathways for tritium production come from reactions in the boron control rods and burnable absorbers as well as the helium coolant. Lithium and boron impurities naturally occurring in graphite add another more avoidable means of tritium production which should be minimized as much as possible [8, 9]. Table 2 gives the important reaction rates to be calculated along with their MT number identifier and availability within the SCALE 6.1 shielding libraries used in the study. Unavailable cross sections were manually inputted from the JENDL-4.0 library [10].

One of the pathways for tritium production in boron is the two-step reaction ^{10}B(n,α)^{7}Li(n,nα)t shown in Table 2. The production rate is time-dependent and based on the production of ^{7}Li via ^{10}B. A set of rate equations involving the production and depletion of each isotope must be considered to derive the total net time-dependent reaction rate. The depletion of boron is written without production or decay and the concentration of the stable isotope ^{7}Li with production from ^{10}B would respectively be,

$$\begin{aligned} \frac{dN_{10B}(t)}{dt} &= -\phi\sigma_{10B,a}N_{10B}(t) \\ \frac{dN_{7Li}(t)}{dt} &= \phi\sigma_{10B(n,\alpha)7Li}N_{10B}(t) - \phi\sigma_{7Li,a}N_{7Li}(t). \end{aligned} \tag{1}$$

These coupled differential equations can be solved by taking each equation's Laplace Transformation,

$$\begin{aligned} s\widetilde{N}_{10B}(s) - N_{10B}(0) &= -\phi\sigma_{10B,a}\widetilde{N}_{10B}(s). \\ s\widetilde{N}_{7Li}(s) - N_{7Li}(0) &= \phi\sigma_{10\mathrm{B}(n,\alpha)7\mathrm{Li}}\widetilde{N}_{10B}(s) - \phi\sigma_{7Li,a}\widetilde{N}_{7Li}(s). \end{aligned} \tag{2}$$

Substituting the ^{10}B term ($\widetilde{N}_{10B}(s)$) from the first equation into the second gives the transformed ^{7}Li concentration only dependent on initial concentrations. In order to take the inverse Laplace transform of this equation, it is rewritten using partial fraction decomposition as,

$$\begin{aligned} \widetilde{N}_{7Li}(s) = &\frac{N_{7Li}(0)}{s+\phi\sigma_{7Li,a}} + \frac{\phi\sigma_{10\mathrm{B}(n,\alpha)7\mathrm{Li}}N_{10B}(0)}{(\phi\sigma_{7Li,a})^2 + (\phi\sigma_{10B,a})^2} \\ &\times(\phi\sigma_{10Ba} - \phi\sigma_{7Lia})\left(\frac{1}{s+\phi\sigma_{7Li,a}} - \frac{1}{s+\phi\sigma_{10B,a}}\right). \end{aligned} \tag{3}$$

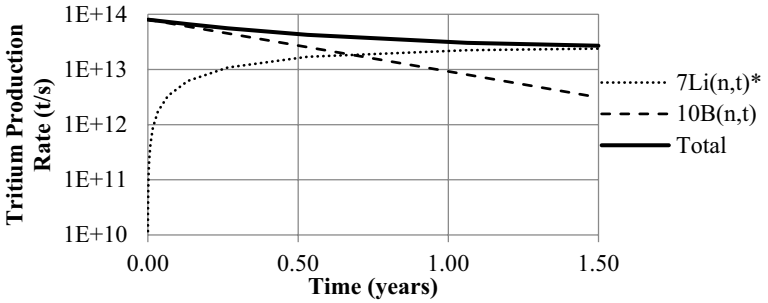

Figure 3. Tritium production rate versus time in burnable absorbers from two coupled reaction rates.

Finally, taking the inverse Laplacian of both sides of the equation yields the time-dependent ^{7}Li concentration to be,

$$N_{7Li}(t) = N_{7Li}(0)\, e^{-\phi\sigma_{7Li,a}t} + \frac{\phi\sigma_{10\mathrm{B}(n,\alpha)7\mathrm{Li}} N_{10B}(0)}{\left(\phi\sigma_{7Li,a}\right)^2 + \left(\phi\sigma_{10B,a}\right)^2} \times \left(\phi\sigma_{10B,a} - \phi\sigma_{7Li,a}\right)\left(e^{-\phi\sigma_{7Li,a}t} - e^{-\phi\sigma_{10B,a}t}\right). \quad (4)$$

The tritium-producing reaction rate is simply (with $N_{7Li(t)}$ from Eq. (4),

$$R = \phi\sigma_{7Li(n,nt)\alpha} N_{7Li}(t). \quad (5)$$

Using the derivation for tritium production rates, the total production rate as a function of time for ^{10}B and ^{7}Li can be solved using a steady-state initial reaction rate. Table 3 shows how the reaction rate would vary with time within burnable absorbers based on the solution given in Eqs. ((1)–(5)). Ideally, fluence rates from shielding calculations would be used in a depletion code to find tritium production rates in two-step reactions instead of solving by hand. However, for this study such analysis was not implemented.

4. Calculating Tritium Production Rates

4.1 Use of FW-CADIS Methodology in MAVRIC in Support of Obtaining Accurate 3D Tritium Production Distribution

For accurate determination of tritium production, we use detailed Monte Carlo simulations, aiming to generate 3D reaction rate distributions. This requires obtaining results ‘everywhere’ with acceptable statistics. The FW-CADIS methodology [11, 12] seeks to bias an MC simulation so that uniform statistics are obtained over a volume of interest. It accomplishes this task by first obtaining both a forward and an adjoint deterministic solution of the problem space. The adjoint fixed-source is given as a desired response to calculate over a given region. In the FW-CADIS methodology the source is inversely proportional to the forward flux. The adjoint discretized solution is then used to form an importance map which biases both the sampling of the forward fixed source and the particle transport during an MC simulation. Ideally, the MC method gives the most accurate results since it is able to preserve an accurate representation of the geometry of the problem as well as continuous energy in nuclear data.

The MAVRIC sequence [13] of the SCALE 6.1 code package implements the FW-CADIS methodology by using Denovo to obtain an S_N (discrete ordinates) solution for the forward flux and adjoint function. MAVRIC creates an importance map from the adjoint function to be used in the fixed-

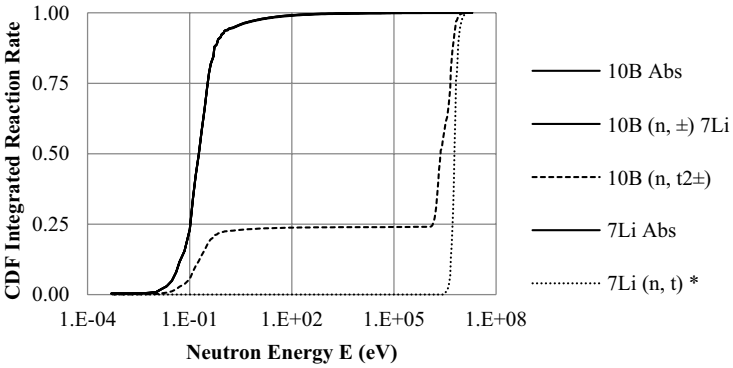

Figure 4. A CDF of tritium-producing reaction rates in boron and lithium.

source MC sequence, using the Monte Carlo code Monaco [13]. One useful aspect of the methodology is the deterministic forward flux only needs to be solved once and then different adjoint functions can be used for importance maps directed at biasing particles to separate adjoint sources, i.e., different responses (reaction rates) of interest. Minimal input is required by the user to accomplish a wide range of simulations, and full advantage was taken of this adaptability.

Separate MAVRIC simulations were performed for each tritium pathway. The problem space spanned $800\times800\times1388.4\,\mathrm{cm}^3 = 889\,\mathrm{m}^3$, had a meshing of $140\times140\times238$ (4.9 million voxels), used a Legendre polynomial and quadrature set of P_3S_8 and employed a 27-group neutron library. Each solution used 16 processors with a maximum solution time of 1.45 hours for each forward and adjoint solution. The MC portion of the MAVRIC sequence was allowed to run for 12 hours for each case using a 200-group neutron library. The group structure is optimized for shielding studies, which generally need more resolution for faster neutrons that stream through shielding materials [63 fast groups (1 MeV–20 MeV); 111 epithermal groups(1 eV–1 MeV); 26 thermal groups (1 eV–1(10^{-5})eV)].

4.2 Issues with Thermal Reactions

The majority of shielding problems focus on the fast neutron fluence (>1 MeV) or reaction rates that have very little contribution from the thermal spectrum. Tritium production however has a large dependence on thermal reaction rates, especially in burnable absorbers and lithium impurities. Figure 4 shows a Cumulative Distribution Function (CDF) of important reaction rates in ^{10}B and ^{7}Li. All reactions exhibit large thermal contributions, except for the ^{7}Li(n,t)*, which has a threshold of 2.86 MeV, and the ^{10}B(n,t2α) which has roughly one quarter of the total contribution in the thermal range.

For thermal reactions, standard MC works fine in obtaining statistically converged results within the burnable absorbers and control rods. However, solving for thermal reaction rates over the graphite reflector region surrounding the core proved challenging using the FW-CADIS methodology. Figure 5 shows the relative uncertainty in ^{10}B(n,α)^{7}Li reaction rate distribution from a MAVRIC simulation with the adjoint source defined as that reaction within all graphite components. The fixed-source is biasing so heavily towards the smallest flux region below the core that very few particles are sampled in the middle and top portions. Here, the FW-CADIS methodology can result in largely inaccurate tallies coupled with an apparently low uncertainty. For example, in the simulation results presented in Fig. 5 the total reaction rate calculated by MAVRIC within all graphite returns $9.0(10^{17}) \pm 10\%$ ($^{7}Li/s$). After using the sectional method described in the next section, the actual tally should be $9.17(10^{18}) \pm 1\%$ ($^{7}Li/s$), which is over an order of magnitude higher. Therefore, it is important that the user is aware of the possibility of false convergence to incorrect solutions especially when looking at large tally regions.

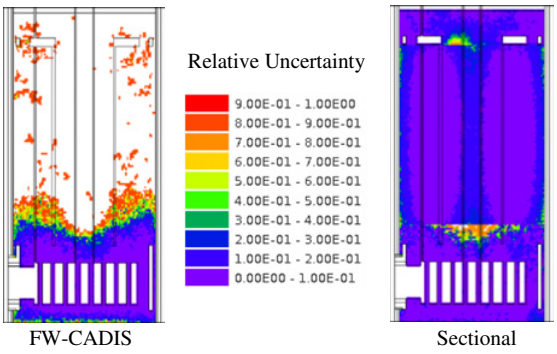

Figure 5. The $^{10}B(n,\alpha)^{7}Li$ reaction rate distribution (left) with its relative uncertainty (right) as calculated by the FW-CADIS method with MAVRIC using a sectional method.

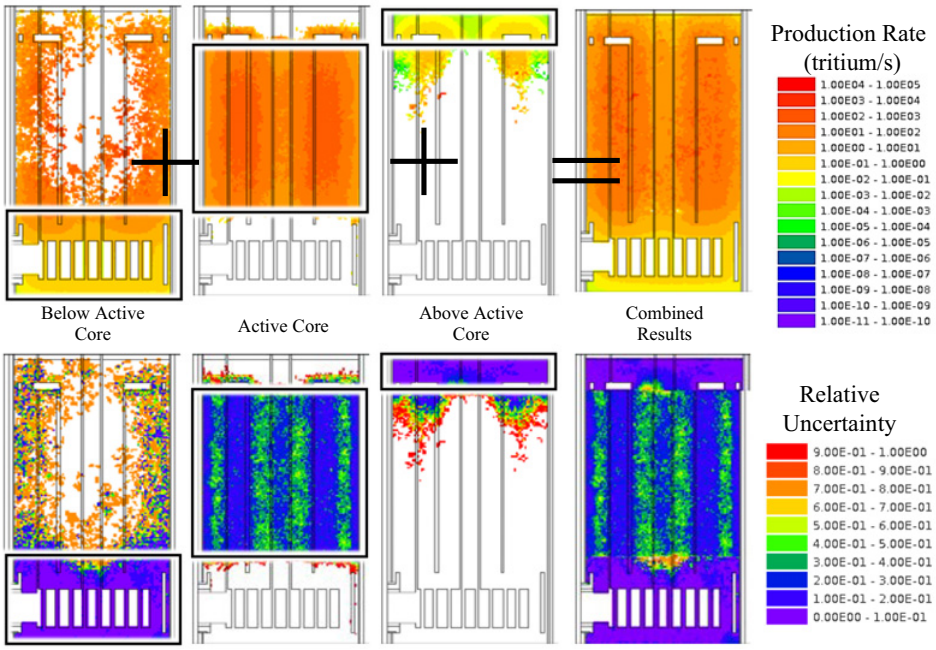

Figure 6. Illustration of the sectional method used to obtain the $^{10}B(n,\alpha)^{7}Li$ reaction rate distribution. Labels indicate the area that was used as the adjoint source when calculating an importance map used for biasing particles.

4.3 A Sectional Method

In order to overcome the issues discussed above with thermal reactions, a sectional method is proposed. Instead of biasing towards the entire problem space, different sections are used as the adjoint source in separate simulations. For this problem, the volume inside the RPV is divided into three regions: above the active core, the active core, and below the active core. Each region is simulated separately and the results are combined via post-processing into a final result as given in Fig. 6. Note that compared with the case of an adjoint source defined by the entire space (compared in Fig. 5), the majority of the problem has converged statistics resulting in both a more accurate and a more precise solution.

Table 3. Tritium production rates from a previous study (left) and from the current study (right).

	(A) Assumed values from (Oh & Kim, 2011)		(C) Calculated values using MAVRIC (this study)		
Pathway	**Activity (Bq/y)**	**Production (t/s)**	**Activity (Bq/y)**	**Production (t/s)**	**Ratio (C/A)**
Ternary Fission	1.03E+14 (62.0%)	1.83E+15	1.03E+14 (29.8%)	1.83E+15	1.00
From ^{10}B	1.49E+13 (9.0%)	2.65E+14	5.00E+13 (14.5%)	8.89E+14	3.36
Control Rod	1.16E+13 (7.0%)	2.06E+14	4.35E+13 (12.6%)	7.74E+14	3.75
Absorber	1.66E+12 (1.0%)	2.94E+13	4.51E+12 (1.3%)	8.02E+13	2.72
Reflector	*1.66E+12 (1.0%)*	*2.94E+13*	*2.00E+12 (.6%)*	*3.56E+13*	*1.21*
From ^{3}He	*2.98E+13 (18.0%)*	*5.30E+14*	*1.43E+13 (4.1%)*	*2.53E+14*	*0.48*
From ^{6}Li	*2.32E+13 (14.0%)*	*4.12E+14*	*1.78E+14 (51.6%)*	*3.16E+15*	*7.67*
Core Graphite	*3.31E+12 (2.0%)*	*5.89E+13*	*5.45E+13 (15.8%)*	*9.68E+14*	*2.74*
Core Matrix	*1.66E+13 (10.0%)*	*2.94E+14*			
Reflector	*3.32E+12 (2.0%)*	*5.88E+13*	*1.23E+14 (35.8%)*	*2.19E+15*	*37.24*
Total	1.71E+14 (100%)	3.03E+15	3.45E+14 (100%)	6.13E+15	2.02
Total (Bq/y/MWt)	2.84E+11		5.75+11		2.02

**Production rates in italics are from impurities, while others are inherently resulting from the core design.*
***Percentages in parenthesis give the percentage of the total for each reaction rate.*
**** MC results are tallied over large regions and are converged to less than 1% relative uncertainty.*

5. Results

Combining all pathways for tritium production resulted in a production rate of almost twice of the total value obtained in [1] by a simpler model production model. Table 3 gives the total rates from each study for comparison. Results are separated by those inherent in the design (fuel, absorbers and control rods) and those due to impurities in the coolant and graphite components. Impurity concentrations are controllable (even if at a cost), while the inherent ones are assumed to be a fixed amount. From the fixed rates it appears that the production in the control mechanisms was previously underestimated by more than 3 times, which could be due to a different core design. The largest difference between each study came from the production within ^{6}Li impurities in graphite [14], which for this work were assumed to be 7ppb (parts per billion). If this number were to be decreased to 1ppb the contribution from ^{6}Li would drop to only a 10% difference from the previous study, leading to an overall tritium production rate increase of only 12%.

6. Conclusions

The tritium-producing reaction rates throughout the structures within the RRV were calculated employing the capability of MAVRIC to perform many different tailored simulations with minimal input by the user. The majority of production in terms of total tritium occurs in the active core region, which can easily be calculated using the standard MC with no biasing. However, if a converged spatial distribution throughout the entire RPV is desired than standard MC is likely to under sample or completely miss large parts of the problem space. If the goal is to obtain an overall reaction-rate spatial distribution than FW-CADIS should be used, but it proved to be problematic when applied to thermal reactions throughout the VHTR model. The large problem space below the bottom reflector

containing the outlet plenum led to a biased source distribution that very heavily sampled particles in the bottom portion of the fixed-source. The adjoint function in the bottom of the core was orders of magnitude higher than that in the center. The biased source is sampled proportionally to the adjoint function, leading to the middle and upper portions of the problem having very few particles sampled in those regions. For finding rates in the core standard MC should be used. For finding fast reaction rate everywhere within the RPV, FW-CADIS was the most effective. For finding thermal reaction rates everywhere, a "sectional method" combining results from FW-CADIS and standard MC proved the most effective. Finally if seeking only the total reaction rate, the CADIS methodology should give the best results and future work would verify this assumption.

With the combined results, the total tritium production calculated using MAVRIC was found to be larger than predicted in previous studies that used a homogenized reactor. Presence of impurities in helium and graphite can greatly influence the final result and should be mitigated as much as possible in the final design.

The knowledge obtained in this study will also be used in tritium production studies related to liquid salt cooled reactors (LSCRs). Moreover, it will inform selection of appropriate dosimetry materials and reactions needed to validate simulations. Additionally, future studies should combine MAVRIC results for neutron fluence rates in different materials with a depletion code in order to more accurately calculate time-dependent production rates based on changing isotopics.

References

[1] C.H. Oh & E.S. Kim, "Scoping Analyses on Tritium Permeation to VHTR Integrated Industrial Application Systems", INL/EXT-10-19607 (March, 2011)

[2] H. Ohashi & S. Sherman, "Tritium Movement and Accumulation in the NGNP System Interface and Hydrogen Plant", INL/EXT-07-12746 (June 2007)

[3] A. Shenoy, "NGNP and Hydrogen Production Preconceptual Design Studies Report", Document 911107, Rev. 0, General Atomics (July 1997)

[4] D. Petti, "NGNP Research and Development Status", INL/EXT-10-19259 (August 2010)

[5] General Atomics, "GT-MHR Conceptual Design Description Report", Document 910720, Rev. 1 (July 1996)

[6] K. Partain, J. Saurwein & A. Shenoy, "Preconceptual Engineering Services For the Next Generation Nuclear Plant (NGNP) with Hydrogen Production", Document 911107, Rev. 0, General Atomics (July 2007)

[7] D. Ilas (personal communication 2011)

[8] E.L. Albenesius, "Tritium as a Product of Fission", Physics Review Letter, **Vol. 3**, pp. 274–275 (September 1959)

[9] D.G. Jacobs, "Sources of Tritium and its Behavior upon Release to the Environment", ORNL/NSIC-37 (December 1968)

[10] K. Shibata, 0. Iwamoto, T. Nakagawa, N. Iwamoto, A. Ichihara, S. Kunieda, …J. Katakura, "JENDL-4.0: A New Library for Nuclear Science and Engineering", *Journal of Nuclear Science Technology*, Vol. **48**(1) (2011)

[11] J.C. Wagner & A. Haghighat, "Automated Variance Reduction of Monte Carlo Shielding Calculations Using the Discrete Ordinates Adjoint Function", *Nuclear Science and Engineering,* Vol. **128**, pp. 186–208 (1998)

[12] J.C. Wagner, E.D. Blakeman & D.E. Peplow, "Forward-Weighted CADIS Method for Global Variance Reduction", *Transactions of the American Nuclear Society*, Vol. **97**, pp. 630–633 (2007)

[13] D.E. Peplow, "MAVRIC: MONACO with Automated Variance Reduction using Importance Calculations", ORNL/TM-2005/39, UT-Battelle, LLC. Oak Ridge National Laboratory (2009)

[14] J.P. Strizak, T.D. Burchell & W. Windes, "Status of Initial Assessment of Physical and Mechanical Properties of Graphite Grades for NGNP Applications", ORNL/TM-2006/553 (September 2006)